JOURNAL OF PROPULSION AND POWER
Vol. 14, No. 6, November–December 1998

Experimental Investigation of a Supersonic Combustion Solid Fuel Ramjet

Abraham Cohen-Zur* and Benveniste Natan†
Technion—Israel Institute of Technology, Technion City, 32000 Haifa, Israel

An experimental parametric investigation of a solid-fuel supersonic combustion chamber in a scramjet configuration was conducted. A hydrogen-burning vitiated air heater was designed and built to simulate flight conditions of Mach 5.5 in high and medium altitudes in a static test facility (stagnation temperatures and pressures of up to 1500 K and 50 atm, respectively). Flow and combustion phenomena were studied by pressure measurements along the fuel grain and by analyzing video images, digitized from the video recording of each test. Self-ignition and flameholding characteristics were consistent with results from previous works. Flow and combustion characteristics changed as inlet conditions extended, exhibiting initially choked or unchoked flow patterns. In the parametric investigation, incoming airflow conditions (total pressure, total temperature, and mass flow rate) defined the parametric space, yielding a regression rate power law of these parameters. Combustion efficiency was found to decrease with the increase of each of the inlet parameters. Increasing the diversion semiangle of the diverging section of the solid grain resulted in lower regression rate values.

Nomenclature

A = cross-sectional area
a = constant
C_p = specific heat in constant pressure
d, D = diameter
F = thrust force
G = mass flux
h = enthalpy
L = fuel grain length
M = Mach number
$\dot{m}$ = mass flow rate
P = pressure
R = gas constant
$\dot{r}$ = fuel regression rate
T = temperature
t = time
u = velocity
x = axial distance
α = diversion semiangle of fuel grain diverging section
γ = ratio of specific heats
η = efficiency
ρ = density
φ = equivalence ratio

Subscripts
a, Air = air
e = exit
exp = experimental
in = inlet
t = total
th = theory

Superscripts
b, c, d = exponents in empirical regression rate law

Presented as Paper 97-3237 at the AIAA/ASME/SAE/ASEE 33rd Joint Propulsion Conference, Seattle, WA, July 6–9, 1997; received Oct. 3, 1997; revision received May 8, 1998; accepted for publication May 26, 1998.

*Graduate Student, Faculty of Aerospace Engineering.
†Senior Lecturer, Faculty of Aerospace Engineering. Senior Member AIAA.

Introduction

As the flight Mach number is increased beyond the area of Mach 5, the hypersonic phenomena that begin to occur significantly reduce the performance of conventional ramjet engines with a subsonic-flow combustion chamber. Reduction of the flow velocity from these high Mach numbers to subsonic ones, ordinarily by passing through several oblique shocks and a normal shock, results in a considerable increase in the flow static temperature as well as in a significant reduction in total pressure. The first poses a problem because only a limited amount of heat can be added to the flow before the dissociation temperature is reached, whereas the latter is purely a loss to the flow thrust potential. In supersonic-combustion ramjet engines (scramjets), the absence of a normal shock in the diffuser leads to lower static temperatures and higher total pressure recovery, compared with conventional ramjet motors, thus making the scramjet the preferable propulsion system for hypersonic flight missions. Figure 1[1] shows a comparison between the evaluated specific impulse of several air-breathing jet engines vs flight Mach number, indicating the scramjet higher performance in hypersonic flight. The scramjet engine holds additional advantages over the conventional ramjet: To accelerate the flow in a ramjet back to supersonic velocities, the flow must be choked in a converging–diverging nozzle that poses a limitation on the maximum total mass flow. This limitation does not exist in the solely diverging nozzle in scramjet engines, allowing larger total mass flow rates. The diverging scramjet nozzle is also advantageous as it is lighter and does not suffer from severe heat fluxes existing in nozzle throats. Another advantage is associated with the low motor static pressure that arises, resulting in lower structural stresses.

The use of solid fuels is widespread in conventional ramjet engines, providing it with desirable characteristics: high-energy density resulting in a more compact system, simplicity (no need for fuel tanks and feeding systems), safety, easy storage for long duration and, finally, readiness upon demand. Consequently, the solid-fueled scramjet engine should extend the operating limits of solid fuel-oriented vehicles, such as missiles, boosters, sustainers and projectiles, into the hypersonic flight regime.

Schematic illustrations of the conventional (subsonic combustion) solid fuel ramjet (SFRJ) and the solid fuel scramjet are presented in Fig 2.

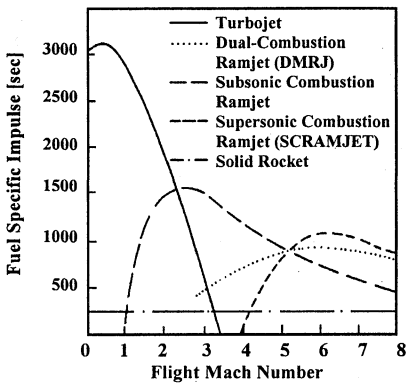

Fig. 1 Evaluation of specific impulse vs Mach number for different jet engines employing hydrocarbon fuel.

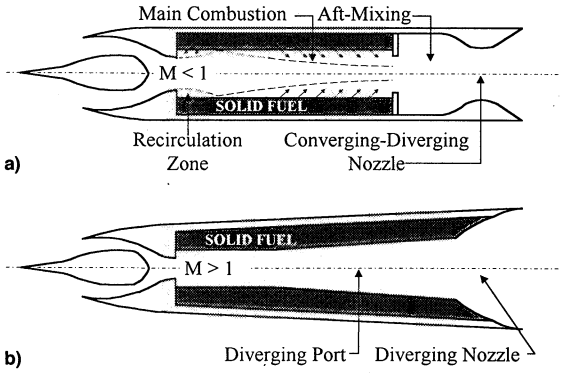

Fig. 2 Configuration of a) subsonic and b) supersonic combustion solid fuel ramjets.

Recent interest in hypersonic vehicles has revived research in the field; however, almost all supersonic combustion research has focused on liquid fuels. Reports related to solid fuel scramjet research, theoretical or experimental, are quite scarce in the open literature.

It is important to mention two experimental studies: Angus et al.[2] were the first to demonstrate, in principle, the combustion of a solid fuel under supersonic flow conditions at good combustion efficiencies. Ben-Yakar et al.[3] were the first to achieve spontaneous ignition and stable supersonic combustion of the solid fuel grain with no external aid.

Solid fuel combustion is characterized by certain inherent features that may cause some operational difficulties in the SFRJ[4] and to a greater extent in the solid fuel scramjet[3]: fuel regression rate, fuel-air mixing, reaction kinetics, and flameholding capacity.

The dependence of the fuel regression rate on the port flow characteristics (with a major effect on the air mass flux and temperature) eliminates the ability to directly control the time-dependent fuel mass flow rate and, hence, the fuel-to-air ratio and the overall fuel consumption. The solid fuel regression changes the combustion chamber geometry, affecting the flow and overall performance of the engine. These phenomena call for a predetermined mission profile. Jarymowycz et al.[5] conducted a numerical study of the combustion of a solid fuel grain under supersonic crossflow. They concluded that combustion takes place in the gas phase above the fuel surface and that the fuel regression rate is affected by the incoming air temperature and to a lesser extent by the pressure. The temporal and spatial fuel regression rates of a poly-methyl-methacrylate (PMMA) solid fuel as a function of the air mass flow rate were measured by Ben-Yakar et al.[3] The average regression rate showed dependence on the airflow rate to the 0.8 power, indicating that the process is dominated by forced-convection heat transfer.

Combustion efficiency may be compromised because of incomplete mixing between the fuel gases emerging from the wall and the air diffusing from the core flow. In supersonic flows, the thinner boundary layer may even further suppress the fuel-air mixing, resulting in even lower efficiencies. Nevertheless, the results of the theoretical study of Ben-Arosh et al.[6] indicated that adequate mixing between the fuel and the incoming air can be obtained within the characteristic residence time in the motor (of the order of 1 ms and less). Mixing can be also enhanced as a result of the surface roughness that is characteristic to the solid fuel scramjet.[2,3,7,8]

The chemical kinetics of the gasified hydrocarbon fuel may be too slow compared with the residence time in the supersonic combustor to complete the reaction. The flowfield of a solid fuel scramjet motor was investigated theoretically by Ben-Arosh et al.[6,9,10] In a detailed numerical study that assumed a two-step chemical reaction of the combusting flowfield, Ben-Arosh et al. showed that combustion takes place within a subsonic zone in the vicinity of the wall while the main core flow remains supersonic. For the geometry chosen (sudden expansion with a constant area hollow fuel grain), theoretical combustion efficiencies in the range of 0.7–0.9 were exhibited.

In SFRJs, flameholding is achieved by a backward-facing step, creating a recirculation zone. This zone is characterized by relatively low velocities, high temperatures, and high fuel concentrations, and it serves as a continuous ignition source. In supersonic combustion SFRJs, the sudden expansion of the flow after the step results in a drop in temperature as well as an increase in the velocity. Furthermore, the reattachment length is shorter in supersonic than in subsonic flows.[10] Under these constraints, it may be concluded that in a solid fuel scramjet with a sudden expansion, flameholding is compromised and residence time is shorter. Defining a flameholding zone consisting of a backward-facing step and a convergence to a desired port diameter can reduce the acuteness of these phenomena. The cavity length actually redefines the recirculation zone length and the port Mach numbers are relatively lower. In this case, internal port dimensions should be designed carefully to avoid thermal choking and maintain supersonic flow throughout the operation. In the experimental study of Angus et al.[2] the combustor internal geometry was based on such a flame stabilization zone that consisted of a sudden expansion of the inlet flow and a cavity in the fuel upstream end. A diverging port combustor section in the downstream end was used to prevent thermal choking. However, under the experimental operating conditions (an inlet stagnation temperature of about 500 K), flame stabilization required injection of a small amount of gaseous hydrogen. Recognizing the special conditions of the supersonic flow, a modified flame-stabilization zone has been suggested by Ben-Yakar et al.[3,8] The flameholding geometry consisted of a constant cross-sectional region in the foremost part of the fuel bounded by an inlet backward-facing step in the upstream direction and an inclined forward-facing step in the downstream side. The flameholding geometric parameters were investigated and actual flameholding limits were established.

The present research objectives were to deepen the understanding of the supersonic combustion of a solid fuel in a scramjet configuration and to form empirical relations regarding the operation and behavior of solid fuel scramjet engines. This is done by measuring the influences of the solid fuel grain geometry and the combustion chamber inlet flow conditions on overall combustion chamber performance, and particularly on its internal ballistics (regression rates and combustion efficiencies). To reach these goals an experimental parametric investigation was conducted in a dedicated connected-pipe static test facility that was designed and constructed to extend the boundaries of the simulated flight envelope beyond what was achieved to date. Figure 3 shows the flight conditions, simulated in the present investigation, compared with previous works.

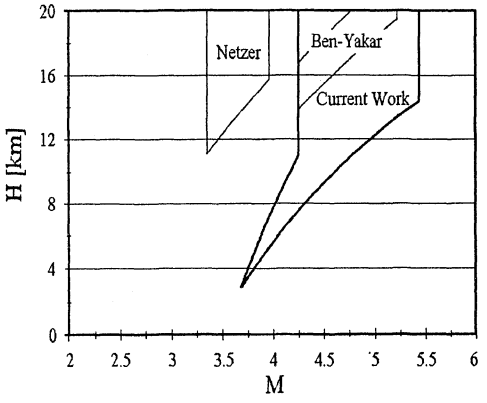

Fig. 3 Simulated flight envelope available in the current research.

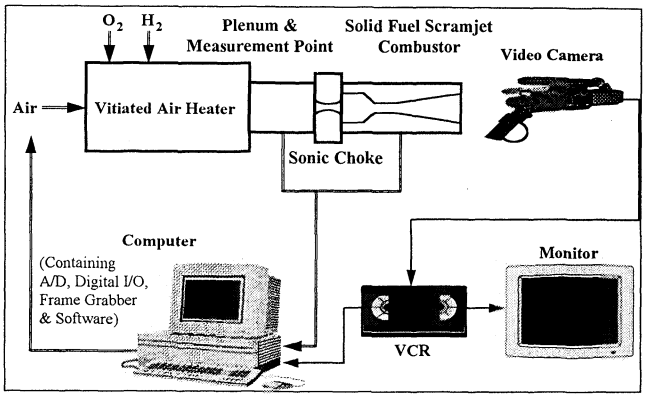

Fig. 4 Schematic diagram of the experimental facility.

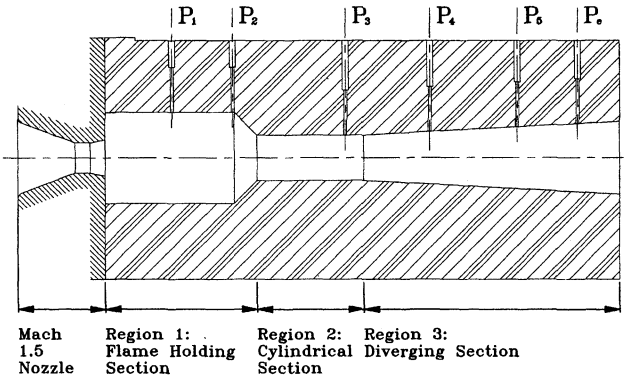

Fig. 5 Schematic of the solid fuel scramjet combustor.

Experimental Apparatus and Procedure

General

The experimental apparatus is shown schematically in Fig. 4. The test facility is composed of three major elements; a vitiated air heater (VAH), a supersonic nozzle, and the tested supersonic solid fuel combustion chamber. Compressed air is provided to the air heater from high-pressure tanks via a flexible conduit and from opposite sides, perpendicular to the motor axis. To keep the oxygen by mole fraction of the vitiated air as in that of natural air (0.209), oxygen is introduced to the flow prior to entering the heater, thus avoiding hazards relating to adding oxygen into a hot flow. The regeneratively cooled vitiated air heater burns hydrogen with the oxygen-enriched air to achieve an inlet total temperature of up to 1500 K, at pressures of up to 50 atm, and mass flow rates of up to 500 g/s. These values simulate an inlet stagnation condition for flight Mach numbers greater than 5.5 at high and medium altitudes.

The supersonic nozzle at the exit of the air heater regulates the airflow rate and accelerates it to Mach 1.5, thus simulating flow conditions at the exit of a generic engine diffuser. The supersonic combustor was made of transparent poly-methil-methacrylate (PMMA–Plexiglas®), which also served as the solid fuel. To obtain correct geometrical measurements, two parallel surfaces were machined on opposite sides of each of the cylindrical grains. The advantage of using Plexiglas, despite its low energetic properties, is that because of its high mechanical strength, there is no need for outer casing and its transparency enables observation of the flow and combustion phenomena within its axisymmetric bore. The solid-fuel grain geometry (Fig. 5) used in this research crystallized from the experimental results of Refs. 2, 3, 7, 8, and 11. It is divided into three regions:

1) A flame-holding section (indexed fh), including a backward-facing step creating a recirculation zone, and a converging section in the shape of an oblique forward-facing step that prevents too high Mach number over the solid fuel surface.

2) A constant diameter cylindrical section (cyl).

3) A long diverging section (div) to maintain supersonic flow with no choking because of the addition of heat and mass. In the previously mentioned studies, this configuration showed good flameholding and combustion stability as well as spontaneous ignition with no need for gaseous reactants to be added to the flow to promote combustion.

Vitiated Air Heater

A hydrogen-burning VAH was designed and constructed to stand the demanding goals of very high pressure and temperature as laid out by the research parameters. The design (Fig. 6) was based on constructing the VAH almost entirely from stainless steel and on a regenerative cooling/ heating configuration, separating the pressure mechanical load-carrying element from the thermal loading.

The VAH is constructed from three major components; an outer shell, an inner combustion chamber, and a nozzle adapter. The outer shell is capable of carrying more than 50-atm gas and is thermally protected by the cold air entering the VAH on the downstream end and moving in the cooling duct backwards, to the upstream end of the VAH. The air enters the VAH perpendicular to its axis to attain a true thrust reading and from opposite sides to cancel side forces. The entrance pipes are offset from the VAH center to provide the flow with tangential momentum to ensure air cooling around the complete outer shell circumference. The inner combustion chamber resembles the classical design, the airflow is divided into a central and a peripheral flow. Hydrogen is impinged into the central airflow to create a close to stoichiometric mixture and the peripheral airflow joins the combustion products through equally distributed holes on the inner liner. The ratio of central to peripheral airflows can be regulated to enable a wide range of operation. The third component serves as an adapter to different nozzles and test sections and as a plenum to complete the hot/cold air mixing. Measurement points are located in the adapter, near the VAH exit. Because the adapter is not externally or internally cooled, it is thermally insulated by a ceramic tube and a ceramic fiber blanket. For the parametric investigation, a series of nine nozzles, all with the same area ratio to provide the same exit Mach number, was designed and fabricated. An additional higher Mach number nozzle was fabricated later to investigate combustion in higher Mach flow.

Data Acquisition and Control

A typical test lasts about 15 s, within which an accurate sequence of functions must be carried out. A computer-controlled automatic system was used to ensure the sequence accurate performance. The same software managed the automated control system via a digital I/O board as well as all data acquisition using an A/D board.

The test facility incorporates several measurement points; static pressure at six points along the solid grain, pressure and temperature at the VAH exit just upstream of the supersonic nozzle, and the trust generated by the VAH/combustor assembly. The mass flow rates of the three gases, air, hydrogen, and makeup oxygen, were measured and regulated, using sonic orifices with upstream pressure and temperature measurements.

A VCR and a video camera were used in all experiments to record the solid fuel grain as combustion progressed. Selected frames from the recordings were then digitized using a video frame grabber PC board to measure regression rates of the solid surface on selected sections along the combustor. Geometrical measurements on the digitized video pictures were conducted using image processing and analysis software. Having the internal port contour data, temporal and spatial variations of the fuel regression rate could be obtained. Overall fuel mass flow rate histories could then be calculated as well.

Results and Discussion

General

A total of 18 successful tests were conducted in four series, each investigating a different parameter: air mass flow rate, stagnation pressure and temperature, and diverging section angle. Grain and nozzle geometry were designed to fall between the flameholding limits established by Ben-Yakar et al.[3] and Ben-Yakar.[8] In addition, the inlet stagnation temperatures were higher than those of Ref. 3; consequently, spontaneous ignition was accomplished, with no use of external means to sustain combustion. The experimental results from all tests are summarized in Table 1.

Flow Characteristics

Information about the flow behavior within the combustor was obtained by the six static pressure measurement points along the grain axis (Fig. 5). In general, two different flow and combustion patterns inside the solid combustor can be distinguished. Figure 7 presents the six pressure-trace histories characteristic to tests in which inlet stagnation pressures are relatively low, or air mass flow rates are relatively high. Figure 8 presents the same data typical to tests with the opposite conditions, i.e., high inlet stagnation pressure or low air mass flow rates. From Fig. 7 it is evident that choking of the flow occurs in the cylindrical section of the solid grain in the first few seconds of operation, causing the high-pressure readings in the flameholding zone. Compared with Fig. 7, Fig. 8 exhibits lower pressures in the flameholding zone than in the cylindrical section, indicating a flow pattern that is supersonic at all times and along the entire grain. To support this theory, the data in Figs. 7 and 8 are reorganized to plot pressure variations along the combustor axis at different times and are presented

Table 1 Summary of selected results from tests divided to parametric groups

Test no.	$T_{t,in}$, K	$P_{t,in}$, atm	$\dot{m}_{in}$, g/s	$\dot{r}$, mm/s	η	φ	Remarks
1	1276	36.9	302	0.81	0.70	0.47	Nominal case:
2	1296	38.2	297	0.74	0.67	0.48	α = 3 deg, $\dot{r}_{div}$ = 0.79
3	1196	21.2	310	0.73	N/A	0.47	
4	1144	21.4	308	N/A	0.83	0.48	Only P_e measured
5	1253	22.5	310	0.73	N/A	0.52	
6	1237	27.6	297	0.76	0.73	0.54	
7	1295	41.6	301	0.77	0.57	0.50	
8	1191	51.6	301	0.85	0.55	0.44	
9	1273	33.1	244	0.68	0.81	0.50	
10	1223	35.8	388	0.98	0.61	0.61	
11	1033	34.8	294	0.66	N/A	0.49	Extinguished after 3 s
12	1186	36.0	294	0.74	0.77	0.46	
13	1364	36.8	301	0.96	0.64	0.53	
14	1247	36.8	304	0.89	0.56	0.49	α = 2 deg, $\dot{r}_{div}$ = 0.96
15	1349	38.6	300	0.82	0.56	0.46	α = 4 deg, $\dot{r}_{div}$ = 0.77
16	1242	37.5	304	0.66	N/A	0.39	α = 5 deg, $\dot{r}_{div}$ = 0.67
17	1298	36.5	293	0.79	0.29	0.43	M_{in} = 1.9

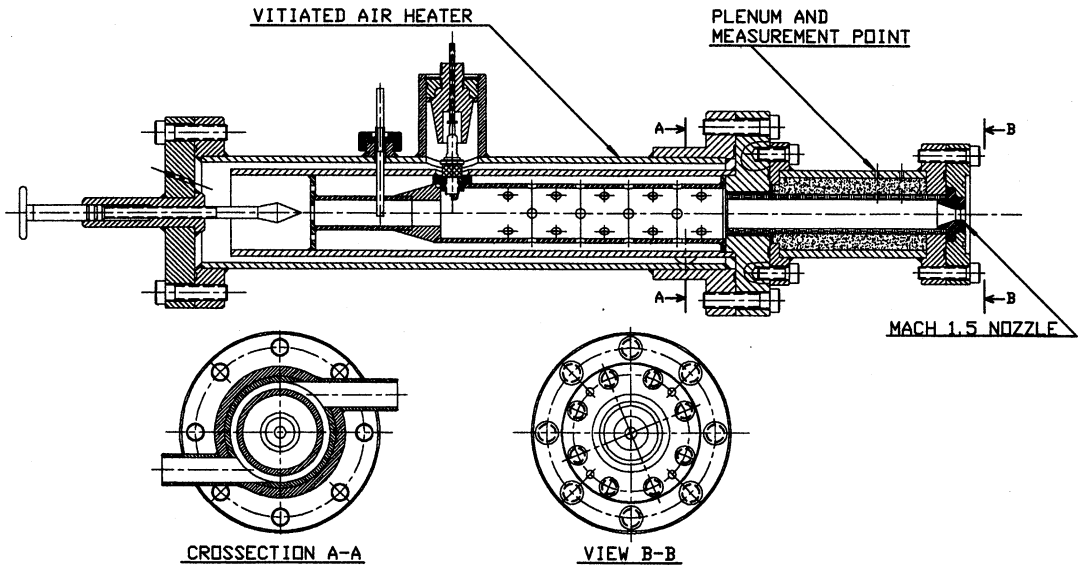

Fig. 6 Facility VAH, cutaway view.

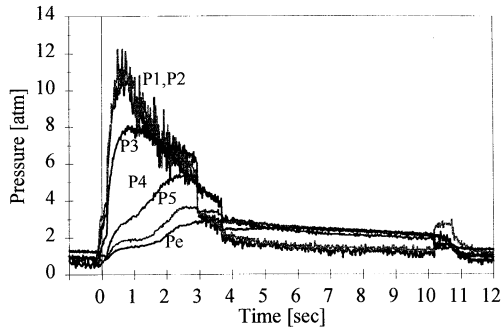

Fig. 7 Wall-pressure traces with time (test no. 3).

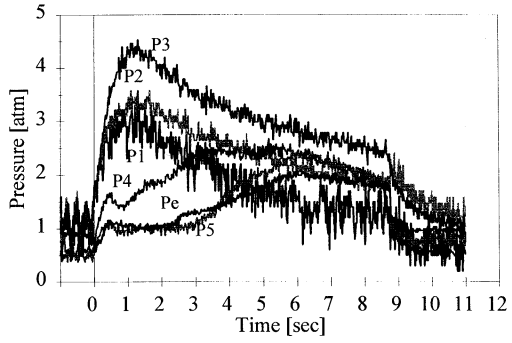

Fig. 8 Wall-pressure traces with time (test no. 1).

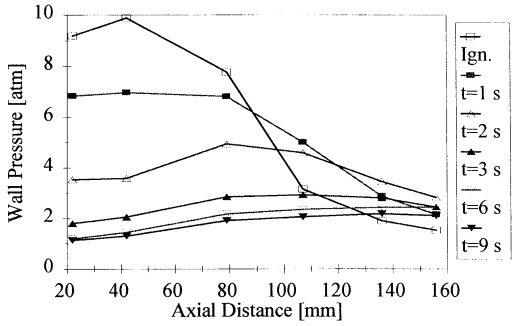

Fig. 9 Temporal variation of wall-pressure distribution along grain axis (test no. 3).

in Figs. 9 and 10, respectively. In the initially choked case (Fig. 9), the pressure is decreasing along the flameholding and cylindrical zones in the first two seconds. Because the grain bore is converging in these zones, the pressure drop characterizes subsonic flow. As the combustion develops, the port area increases and the choke weakens and eventually disappears until a full supersonic flow is exhibited. In Fig. 10 (initially unchoked), the pressure is increasing in the converging part of the grain, indicating supersonic flow throughout the operation. The highest pressure reading is of gauge no. 3, corresponding to the smallest cross-sectional area in the combustor.

The influence of low and high incoming air mass flow rate on the transition between the two flow patterns (initially choked and initially unchoked) is straightforward. However, the influence of the stagnation pressure on the flow pattern needs some explanation. To lower the inlet stagnation pressure, while keeping the mass flow rate, the stagnation temperature, and the Mach number constants, the throat area of the supersonic inlet nozzle connecting the VAH to the solid grain is enlarged. Because the grain geometry is constant, the area ratio between any section of the grain port and the throat is decreased; hence, the flow undergoes a more moderate expansion and the resulting static temperature and pressure are higher than in the case of high total pressure. Thus, in the lower inlet

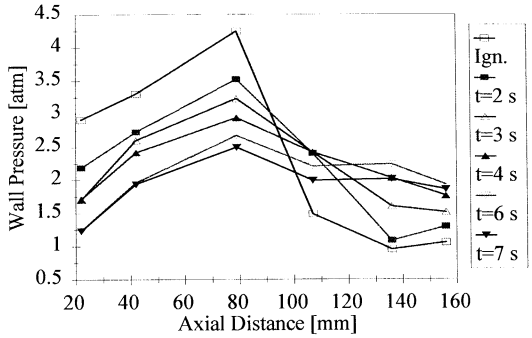

Fig. 10 Temporal variation of wall-pressure distribution along grain axis (test no. 1).

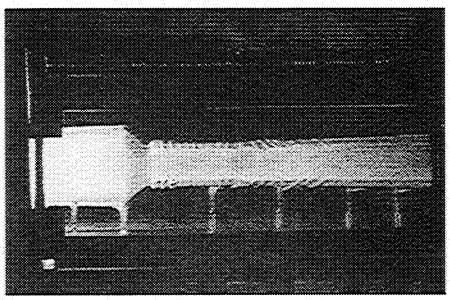

Fig. 11 Shock-train development in the cylindrical section after ignition (test no. 3).

stagnation pressure tests, the flow conditions in the cylindrical section are closer to choking. The addition of heat and mass from the evaporating solid fuel upstream of the choke location complements the requirements for choking.

The overall behavior of the pressure readings in both trends indicate supersonic flow in all other times and locations along the combustor. This is mainly evident by the decreasing of the pressure with time as the port area is increased because of fuel regression. The initially choked flow characteristics correspond well to the experimental results of Ben-Yakar et al.[3] and Ben-Yakar,[8] whereas the all-supersonic, initially unchoked, flow pattern is clearly an entirely new phenomenon.

Finally, the distinct appearance of a shock-train in the cylindrical section and oblique shocks in the diverging section, as seen in Fig. 11 (taken at about 1 s after ignition), and higher than the atmospheric pressure at the combustor exit, serve as additional indications to the supersonic nature of the combustion.

Thermal Efficiency

Combustor thermal efficiency was calculated using a procedure similar to Ref. 2. Thermal efficiency is defined as the ratio between the flow actual and theoretical values of the total enthalpy rise in the combustor. In the evaluation, the enthalpy was approximated, yielding the following expression for the thermal efficiency:

$$\eta_{\Delta h} = \frac{(C_p T_t)_e - (C_p T_t)_{\text{in}}}{(C_p T_{t,\text{th}})_e - (C_p T_t)_{\text{in}}} \tag{1}$$

The theoretical exit total temperature and C_p were calculated using the thermochemical code PEP–CODE.[12] The actual exit static temperature and velocity were calculated from the mass conservation equation

$$\dot{m}_e = \rho_e u_e A_e = P_e M_e A_e \sqrt{\gamma_e / R_e T_e} \tag{2}$$

Table 2 Time-dependent efficiency calculation in a typical test

Time, s	F, kgf	P_e, atm	A_e, cm^2	M_e	U_e, m/s	$T_{t,\text{in}}$, K	T_e, K	$T_{t,e}$, K	φ	$T_{t,e,\text{th}}$, K	η_h
4	35.2	0.97	5.3	2.30	1115	945	614	1037	0.36	1977	0.16
5	37.9	0.90	5.9	2.35	1210	1164	693	1189	0.38	2008	0.14
6	38.0	1.05	6.6	2.05	1181	1231	869	1340	0.40	2039	0.25
7	37.7	1.40	7.2	1.63	1093	1273	1182	1583	0.42	2069	0.48
8	36.8	1.74	7.9	1.31	965	1282	1428	1740	0.44	2099	0.63
9	36.9	1.77	8.7	1.23	940	1293	1543	1838	0.46	2128	0.70
10	36.1	1.67	9.4	1.21	925	1304	1557	1843	0.48	2156	0.69
11	35.0	1.60	10.2	1.16	893	1296	1563	1828	0.50	2183	0.66
12	34.3	1.55	11.1	1.12	871	1306	1598	1851	0.52	2210	0.66

where the exit Mach number was calculated from the thrust measurements assuming perfect gas and momentum conservation described by

$$F = \dot{m}u_e + (P_e - P_a)A_e \tag{3}$$

obtaining the following equation for M_e:

$$M_e = \left[\frac{F - (P_e - P_a)A_e}{\gamma_e P_e A_e}\right]^{1/2} \tag{4}$$

In all of the preceding equations the gas properties γ, R, and C_p were taken from the thermochemical code in the appropriate conditions and all other parameters were measured. It is important to mention that the efficiency values obtained in this procedure are slightly higher than the actual values, as $C_{p,e}$, as taken from the thermochemical code, corresponds to the flow theoretical properties, and are thus higher than in the actual gas. A somewhat lower than the actual value can be derived by assuming a constant C_p. The differences between the two values are rather small, and it is assumed here that the current procedure gives results that are closer to the true values.

Calculation results for a typical test are summarized in Table 2. The resulting time-dependent thermal efficiency of this test is presented in Fig. 12. The thermal efficiency exhibits a transition period of a few seconds at the beginning of the operation, in which it increases steadily from very low values, close to zero, until it reaches steady state of high values, mildly decreasing with time. This calls for the conclusion that the heat transfer from the hot airflow to the solid grain causes fuel regression, thus extracting heat from the flow; however, very little of the evaporating fuel actually burns within the combustor in the initial stage of operation. This phenomenon is probably caused by too brief residence times compared with the mixing and reaction characteristic times. As the flow develops, the velocity decreases because of heat addition (that increases gradually with the velocity decrease) prolonging the residence time thus allowing more fuel to burn within the combustor. Additionally, shock-boundary-layer interactions develop surface roughness, characteristic to supersonic solid fuel combustion,[2,3] enhancing mixing and also decreasing the flow velocity. The result of the preceding mechanism is the gradual increase of the efficiency with the development of the flow. An interesting observation supported the encountered efficiency behavior. In video recordings taken from a distant point of view, it was observed that during the first few seconds of the combustor operation (the time period corresponding to the low efficiency transition state), there was a large and bright plume at the exit of the combustor, indicating that the fuel vapors did not burn inside the motor. Then (as the calculated efficiency rose), the plume shrunk to a small and fainter jet and the combustor interior brightened (as if the plume was drawn back to the motor). This corresponds well to more of the fuel burning inside the combustor. Under these conditions, the analysis focused on the steady state of the combustor operation. Moreover, during steady state the flow is supersonic along the combustor, including the cases where the flow is initially choked.

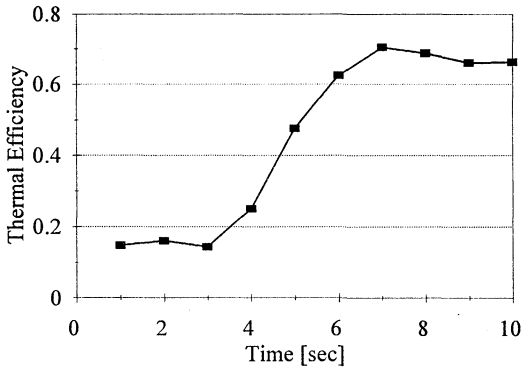

Fig. 12 Combustion thermal efficiency development with time.

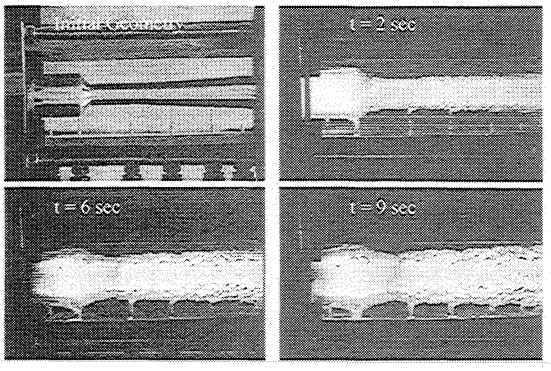

Fig. 13 Sequence of digitized video images of combustion development.

Fuel Regression

The ability to acquire and digitally process and analyze the video images of the burning surface of the transparent Plexiglas fuel permitted continuous visualization of the internal port contour at high spatial and temporal resolution. In Fig. 13, a series of four images, taken in different times during a typical test, demonstrates combustion development and contour variation. Figure 14 presents the variation of the port diameter in time, of a typical test, as measured with the use of an image processing software. At a given time, the local regression rate was calculated from the variation of the port diameter. It was then possible to look at time dependency and axial change of the solid fuel regression rate. The video images were digitized in resolution of less than 0.3 mm/pixel; hence, a single measurement has a rather low accuracy. This is improved as the values under consideration are averages over a large number of measurement points, resulting in a calculated accuracy of less than $\pm 6\%$ in the averaged values.

The flow pattern discussed earlier (initially choked and initially unchoked) apparently influenced the fuel regression rate behavior. In an initially choked test, the regression rate vari-

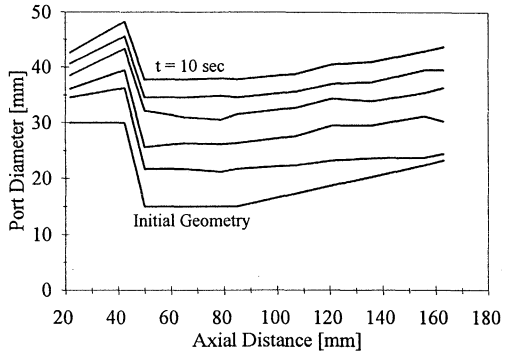

Fig. 14 Variation of the fuel port contours during burning (time intervals of 2 s).

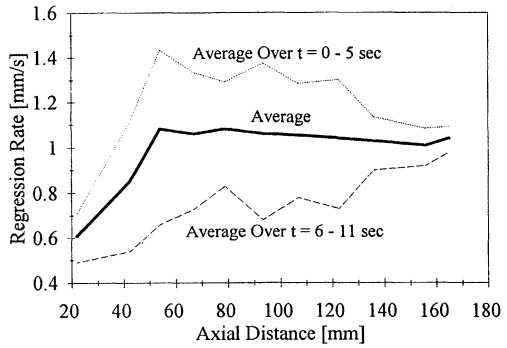

Fig. 15 Axial variation of the time-average local regression rate (test no. 3).

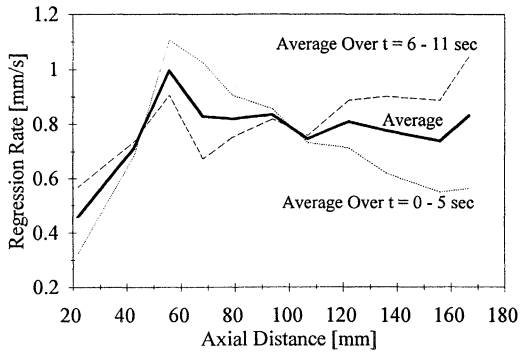

Fig. 16 Axial variation of the time-average local regression rate (test no. 1).

ation along the grain axis is presented in Fig. 15. In addition to the overall time average, the time average of the first and the last 5 s of the operation are also presented. The regression rate appears to reach peak values in the cylindrical section, where mass flux is maximum. It is also evident from the first and the last 5-s traces that the regression rate is decreasing with time, apparently because of the increase of the port area and the resulting decrease in mass flux. Also, the transition from subsonic to supersonic flow in this section reduces the pressure and temperature, which also causes regression rates to decrease. A similar plot is presented in Fig. 16 for an initially unchoked test. The variation along the grain axis remains similar as regression rates are higher at the cylindrical section, but the overall combustor regression rate appears to remain constant in time as the regression rate is decreased in the upstream half of the combustor and increased in the aft half of it. This increase in the aft section of combustor corresponds to the pressure and temperature increase in the flow because of heat addition. The two different behaviors also affect the fuel mass flow-rate time dependency.

Parametric Investigation

A parametric investigation was conducted to evaluate the dependence of the fuel regression rate and combustion thermal efficiency on inlet flow parameters simulating different flight conditions. Apart from the three inlet parameters investigated, air mass flow rate, total pressure, and total temperature, a fourth parameter was investigated, namely the diversion angle of the diverging section in the combustor. As mentioned earlier, only the steady-state values were taken into consideration, as the transition period is assumed to be considerably shorter than the steady-state operation of a combustor in a realistic propulsion system.

In solid fuel ramjet combustors, under both subsonic and supersonic flows, the solid fuel regression rate is often correlated to a function of the incoming air mass flux G, its temperature T, and the chamber pressure P.[4,5,13] The correlation function is usually of the form

$$\dot{r} = a \cdot G^b \cdot T^c \cdot P^d \tag{5}$$

Because the internal geometry, i.e., diameter, varies along the grain axis in the supersonic combustors investigated in this

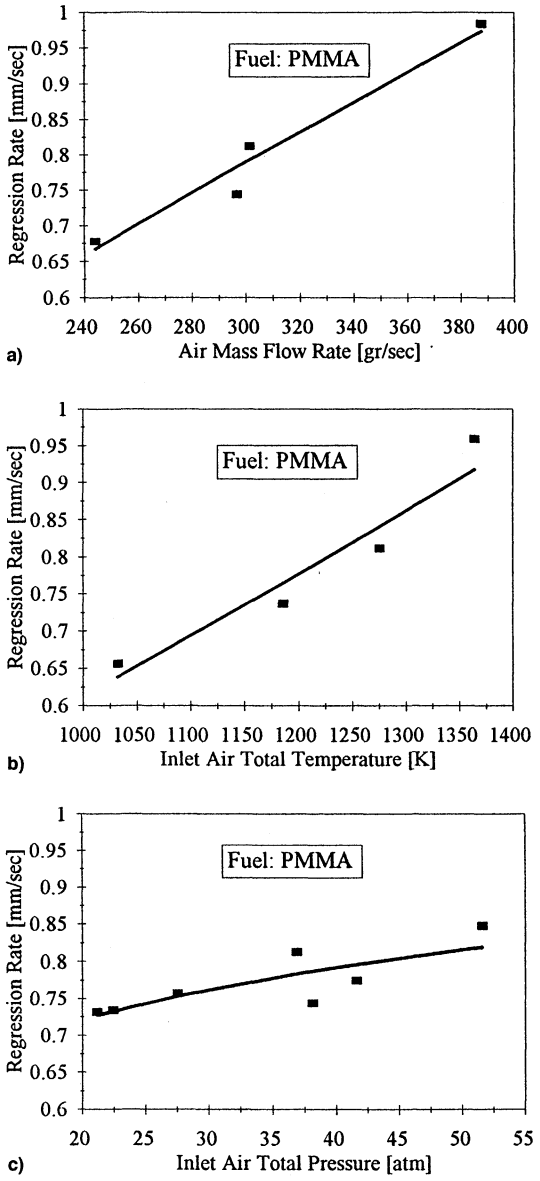

Fig. 17 Regression rate dependence on inlet air parameters: a) mass flow rate, b) stagnation temperature, and c) stagnation pressure.

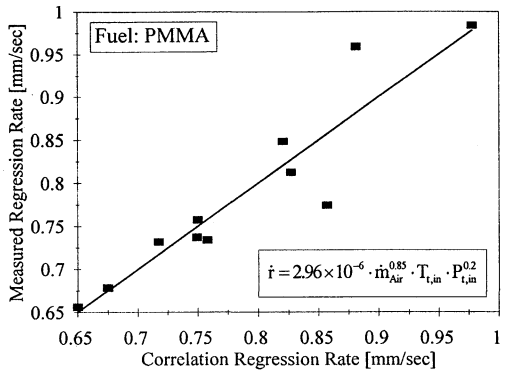

Fig. 18 Test results in comparison with the multivariable power law correlation.

research, the preceding parameters are not constant in the combustor. However, the relating inlet parameters, $\dot{m}_{Air}$, $T_{t,in}$, and $P_{t,in}$ respectively, can be good equivalents to the chamber values. The regression rate was correlated to a function of the following form using a multidimensional regression:

$$\dot{r} = a\cdot\dot{m}_{Air}^{b}\cdot T_{t,in}^{c}\cdot P_{t,in}^{d} \tag{6}$$

In addition, a single parameter dependence in the form of a power law was calculated to verify the parameters overall power law consistency.

Figure 17 shows the single parameter correlations of the three parameters $\dot{m}_{Air}$, $T_{t,in}$ and $P_{t,in}$. Figure 18 presents the correlation accuracy for the overall regression. The resulting regression rate relations obtained are as follows:

The dependence of the regression rate solely on air mass flow rate $\dot{m}_{Air}$, total temperature $T_{t,in}$, and total pressure $P_{t,in}$, can be respectively expressed by

$$\dot{r} = 7.5\times10^{-3}\cdot\dot{m}_{Air}^{0.82} \quad \text{at} \quad T_{t,in}\approx 1270\ \text{K}, P_{t,in}\approx 36\ \text{atm} \tag{7}$$

$$\dot{r} = 7.8\times10^{-5}\cdot T_{t,in}^{1.30} \quad \text{at} \quad P_{t,in}\approx 36\ \text{atm}, \dot{m}_{Air}\approx 300\ \text{g/s} \tag{8}$$

$$\dot{r} = 0.48\cdot P_{t,in}^{0.14} \quad \text{at} \quad T_{t,in}\approx 1250\ \text{K}, \dot{m}_{Air}\approx 300\ \text{g/s} \tag{9}$$

The overall regression rate correlation is expressed by

$$\dot{r} = 2.96\times10^{-6}\cdot\dot{m}_{Air}^{0.85}\cdot T_{t,in}\cdot P_{t,in}^{0.2} \tag{10}$$

In Eq. (10), $\dot{m}_{Air}$ is measured in grams per second, $T_{t,in}$ in K, $P_{t,in}$ in atm, and $\dot{r}$ in mm/s.

It is important to note that the power of $\dot{m}_{Air}$ ($\approx$0.8) is similar to the value obtained by Ben-Yakar et al.,[3] regarding supersonic combustion and to the values obtained for subsonic SFRJ combustors, indicating the dominance of convective heat transfer on the regression rate. The power of $P_{t,in}$ ($\approx$0.2) corresponds to the value obtained by Jarymowycz et al.,[5] who numerically investigated solid fuel combustion under supersonic crossflows. The power of $T_{t,in}$ ($\sim$1) is relatively higher than encountered in the literature.

For thermal efficiencies, Fig. 19 exhibits a general decrease in thermal efficiency with the increase of each parameter. From this result it can be concluded that efficiency decreases with an increasing regression rate, and this is shown in Fig. 20. This is understandable in light of the fact that increasing the regression rate increases fuel mass flow rate as well, considering that during the brief residence time of the flow in the combustor, mixing of the fuel vapors and the core airflow is incomplete. Increasing regression rate introduces more fuel to the flow, only this fuel does not burn inside the combustor, hence, the lower efficiency. Because the calculated accuracy of the thermal efficiency is not very good ($\sim$20%), a mathematical correlation was not evaluated. In a realistic propulsion

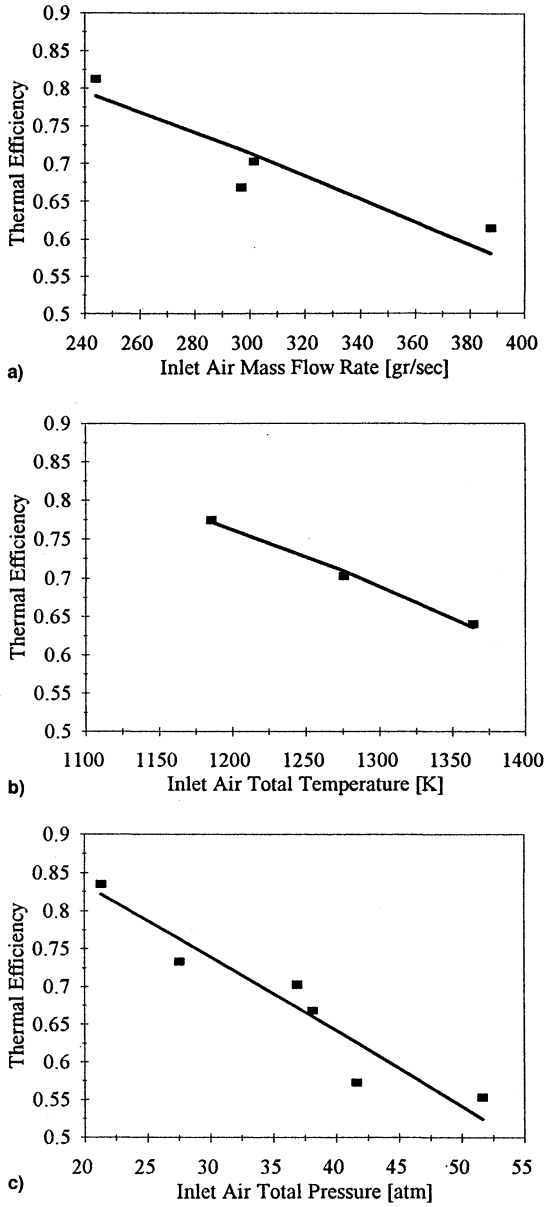

Fig. 19 Combustion efficiency dependence on inlet air parameters: a) mass flow rate, b) stagnation temperature, and c) stagnation pressure.

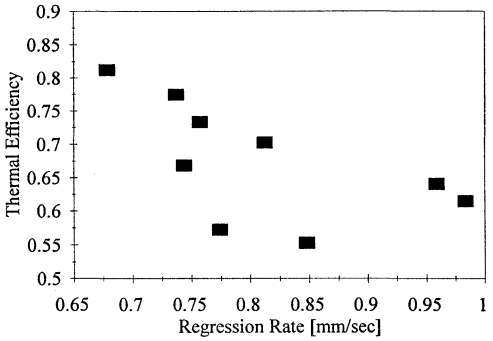

Fig. 20 Efficiency decrease with regression rate increase.

system some measures can be applied to increase the efficiency. The flow residence time can be prolonged by adding an extending section to the combustor at the exit, or mixing can be enhanced by increasing the ratio between the bore circumference and its cross-sectional area, e.g., several small bores rather than one.

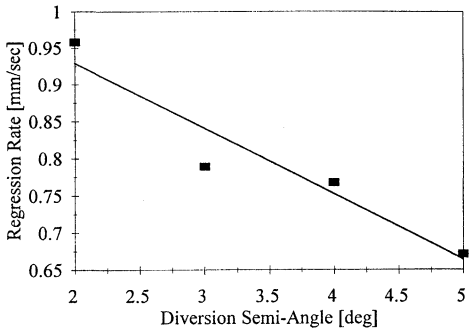

Fig. 21 Regression rate dependence on diversion semiangle of the diverging section.

An additional set of tests was conducted to measure the influence of α in the solid fuel grain. From the video images it is evident that enlarging the diversion angle accelerates the flow in the section and thus decreases the regression rates. At large angles, the flow near the solid fuel surface was darker than at smaller angles, indicating lower temperatures. Figure 21 presents the regression rates measured from the diverging section alone for different diversion angles exhibiting a drop in regression rate as α increases. Efficiency however, most likely exhibits a tradeoff between a decrease because of the increase in the regression rate at low values of α and a decrease because of flow acceleration (shorter residence time) at high α values. Hence, a peak efficiency was received for α = 3 deg (tests 1, 2, 14, and 15), although more tests should be conducted to validate this result.

A final test was conducted to demonstrate combustion in a higher entrance Mach number. A nozzle with an exit Mach number of 1.9 was used. Ignition was spontaneous and combustion sustained throughout the operation, but efficiency was very low (about 0.3).

In general, physical values measurements were fairly accurate in all measurement points. The accuracies of the thrust and exit pressure measurements (<1 and <5%, respectively) have special importance because they effect the combustion thermal efficiency calculation. The other measured parameters that participate in Eqs. (1–4) are more accurate. Nevertheless, the calculated accuracy of the thermal efficiency suffers from the elaborate mathematical expressions, resulting in a somewhat low accuracy of about ±20%.

Concluding Remarks

A solid fuel supersonic laboratory combustor has been tested experimentally in a wide range of inlet conditions. A hydrogen-burning VAH was designed and constructed to provide simulation of a flight Mach number of 5.5 at high and medium altitudes, i.e., total air temperature and pressure of 1500 K and 50 atm, respectively.

Self-ignition of the PMMA solid fuel and flameholding characteristics were consistent with the results of previous works demonstrating solid fuel supersonic combustion.

Two flow and combustion patterns were observed. The initially choked and initially unchoked flows exhibited different trends in the regression rate and, hence, fuel mass flow rate development with time.

The initially unchoked flow pattern was encountered for the first time in the present research. This combustion behavior apparently results from the extension of the operating parameters beyond the previously tested region. Evidently, supersonic combustion of solid fuels can be accomplished without the need of thermal choking in the beginning of the combustor operation. The appearance or absence of thermal choking depends on the geometry and the incoming air conditions.

A low efficiency transition period was detected at the beginning of each test as a result of high velocities and insufficient mixing. This transition period was assumed to be negligibly short in a realistic propulsion system, but it must be taken into consideration for short operating time systems.

A parametric investigation was conducted to determine the effect of the incoming air conditions and grain geometry as combustion characteristics. A regression rate power law was obtained that was consistent with results from previous works. A dependency of the regression rate on the incoming air mass flow rate to the power of 0.85 indicates the importance of forced convection heat transfer in the fuel pyrolysis process.

Combustion thermal efficiency was found to decrease with an increase of any parameter increasing regression rate, supporting the assumption of insufficient mixing and residence time. Measures can be taken to improve the situation.

An indication to the existence of an optimal diversion angle that results in a maximal combustion efficiency was found.

Spontaneous ignition and sustained combustion were obtained in entrance Mach numbers as high as 1.9.

As this research focused mainly on the operational characteristics of the supersonic combustion chamber of a scramjet engine, the obtained results are general and are valid inside a large operational domain of an entire scramjet engine. The choice of the other engine components (diffuser, nozzle), and the flight conditions (M, H), will determine the engine performance and, hence, its applicability in a desired propulsion system. Based on the current research results, and considering the combustor as a component in a designed engine for specified flight conditions, simplified performance calculations yielded relatively high I_{sp}, though expectedly lower than liquid fuel scramjets. The performance was better at higher altitudes. These assessments confirm the potential of solid fuel scramjets as worthy candidates for the types of propulsion systems discussed.

References

[1]Vaught, C., Witt, M., Netzer, D., and Gany, A., "Investigation of Solid-Fuel, Dual-Mode Combustion Ramjets," *Journal of Propulsion and Power*, Vol. 8, No. 5, 1992, pp. 1004–1011.

[2]Angus, W. J., Witt, M. A., Laredo, D., and Netzer, D. W., "Solid Fuel Supersonic Combustion," *La Recherche Aerospatiale*, No. 6, 1993, pp. 1–8.

[3]Ben-Yakar, A., Natan, B., and Gany, A., "Investigation of a Solid Fuel Scramjet Combustor," *Journal of Propulsion and Power*, Vol. 14, No. 4, 1998, pp. 447–455.

[4]Zvuloni, R., Levy, Y., and Gany, A., "Investigation of a Small Solid Fuel Ramjet Combustor," *Journal of Propulsion and Power*, Vol. 5, No. 3, 1989, pp. 269–275.

[5]Jarymowycz, T. A., Yang, V., and Kuo, K. K., "Numerical Study of Solid-Fuel Combustion Under Supersonic Crossflows," *Journal of Propulsion and Power*, Vol. 8, No. 2, 1992, pp. 346–353.

[6]Ben-Arosh, R., Natan, B., Spiegler, E., and Gany, A., "Mixing of Supersonic Airflow with Fuel Added Along the Wall in a Sudden Expansion Chamber," AIAA Paper 97-3241, July 1997.

[7]Angus, W. J., "An Investigation into the Performance Characteristics of a Solid Fuel Scramjet Propulsion Device," M.S. Thesis, Dept. of Aeronautics and Astronautics, Naval Postgraduate School, Monterey, CA, Dec. 1991.

[8]Ben-Yakar, A., "Investigation of the Combustion of Solid Fuel at Supersonic Conditions in a Ramjet Engine," M.S. Thesis, Faculty of Aerospace Engineering, Technion—Israel Inst. of Technology, Haifa, Israel, May 1995.

[9]Ben-Arosh, R., Natan, B., Spiegler, E., and Gany, A., "The Reacting Flowfield Within a Supersonic Combustion Solid Fuel Ramjet," AIAA Paper 97-3119, July 1997.

[10]Ben-Arosh, R., "Theoretical Investigation of Supersonic Combustion of Solid Fuel in a Ramjet Engine," Ph.D. Dissertation, Faculty of Aerospace Engineering, Technion—Israel Inst. of Technology, Haifa, Israel, April 1997.

[11]Witt, M. A., "Investigation into the Feasibility of Using Solid Fuel Ramjets for High Supersonic/Low Hypersonic Tactical Missiles," M.S. Thesis, Dept. of Aeronautics and Astronautics, Naval Postgraduate School, Monterey, CA, June 1989.

[12]Cruise, D. R., "Theoretical Computation of Equilibrium Composition, Thermodynamic Properties, and Performance Characteristics

of Propellant Systems (PEP Code),'' Naval Weapons Center, China Lake, CA, April 1979.

[13]Ben-Arosh, R., and Gany, A., "Similarity and Scale Effects in Solid-Fuel Ramjet Combustors,'' *Journal of Propulsion and Power*, Vol. 8, No. 3, 1992, pp. 615–623.

[14]Billing, F. S., "Research on Supersonic Combustion,'' *Journal of Propulsion and Power*, Vol. 9, No. 4, 1993, pp. 499–514.

[15]Tsoor, A., "Development of Test Facility for Experimental Study of Thrust Modulation in Ram-Rocket,'' M.S. Thesis, Faculty of Aerospace Engineering, Technion—Israel Inst. of Technology, Haifa, Israel, June 1991.

[16]Swartwout, W., Erdos, J., Engers, R., and Prescott, C., "An Oxidation and Erosion Test Facility for Cooled Panels,'' AIAA Paper 92-5095, Dec. 1992.